THE JOURNAL OF PHYSICAL CHEMISTRY B

Article

pubs.acs.org/JPCB

Hydrogen-Bonding and the Dissolution Mechanism of Uracil in an Acetate Ionic Liquid: New Insights from NMR Spectroscopy and Quantum Chemical Calculations

João M. M. Araújo,*[,†] Ana B. Pereiro,[†] José N. Canongia Lopes,[†,‡] Luís P. N. Rebelo,[†] and Isabel M. Marrucho*[,†,§]

[†]Instituto de Tecnologia Química e Biológica, Universidade Nova de Lisboa, Apartado 127, 2780-157 Oeiras, Portugal

[‡]Centro de Química Estrutural, Instituto Superior Técnico, 1049-001 Lisboa, Portugal

[§]Departamento de Química, CICECO, Universidade de Aveiro, 3810-193 Aveiro, Portugal

Supporting Information

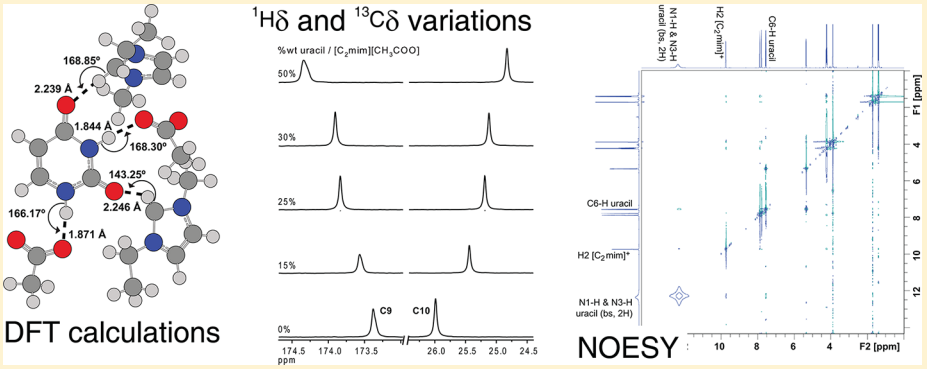

ABSTRACT: The dissolution of uracil—a pyrimidine nucleic acid base—in the ionic liquid 1-ethyl-3-methylimidazolium acetate ([C_2mim][CH_3COO]) has been investigated by methods of ^{1}H and ^{13}C NMR spectroscopy, ^{1}H—^{1}H NOESY NMR spectroscopy, and quantum chemical calculations. The uracil—[C_2mim][CH_3COO] interactions that define the dissolution mechanism comprise the hydrogen bonds between the oxygen atoms of the acetate anion and the hydrogen atoms of the N1—H and N3—H groups of uracil and also the hydrogen bonds between the most acidic aromatic hydrogen atom (H2) of the imidazolium cation and the oxygen atoms of the carbonyl groups of uracil. The bifunctional solvation nature of the ionic liquid can be inferred from the presence of interactions between both ions of the ionic liquid and the uracil molecule. The location of such interaction sites was revealed using NMR data (^{1}H and ^{13}C chemical shifts both in the IL and in the uracil molecule), complemented by DFT calculations. NOESY experiments provided additional evidence concerning the cation—uracil interactions.

1. INTRODUCTION

This decade continued to witness a surge in the field of ionic liquids (ILs) caused by their unique properties and potential uses as green solvents and novel reaction media.[1] ILs are a class of novel liquid salts offering a highly solvating environment in which a number of organic and inorganic solutes may be dissolved.[2,3] This is due to the balance between their ionic nature (dominated by the electrostatic forces between ions) and the possibility of other types of interactions (dispersion, dipolar, hydrogen-bonding) between the ions or between the ions and molecular solvents. Thus, the physical properties of ILs result from the combined properties of their cations and anions, which can be tailored by selecting their nature and structure from a plethora of distinct possibilities. Accordingly, ILs are also called "designer solvents",[4,5] and this fact enables their use in fields as diverse as synthesis and catalysis,[6] electrochemistry,[7,8] biochemistry and dissolution of biomaterials,[9,10] or material engineering.[11]

In pure ILs, there are two types of interactions that are responsible for the liquid structure: the long-range Coulomb interactions, undoubtedly the strongest interactions among the forces between the ions,[12−14] and the short-range dispersion interactions whose importance has recently became clear. Such balance leads in many cases to the formation of nanodomains with peculiar solvation properties.[15,16] Other specific atomic features of the ions of the IL, such as hydrogen-bonding interactions,[17,18] can also lead to secondary structure-directing effects in the liquid phase. The important role that hydrogen bonds perform in the organization and structure of ILs is well-

Received: January 22, 2013
Revised: March 21, 2013
Published: March 22, 2013

 © 2013 American Chemical Society

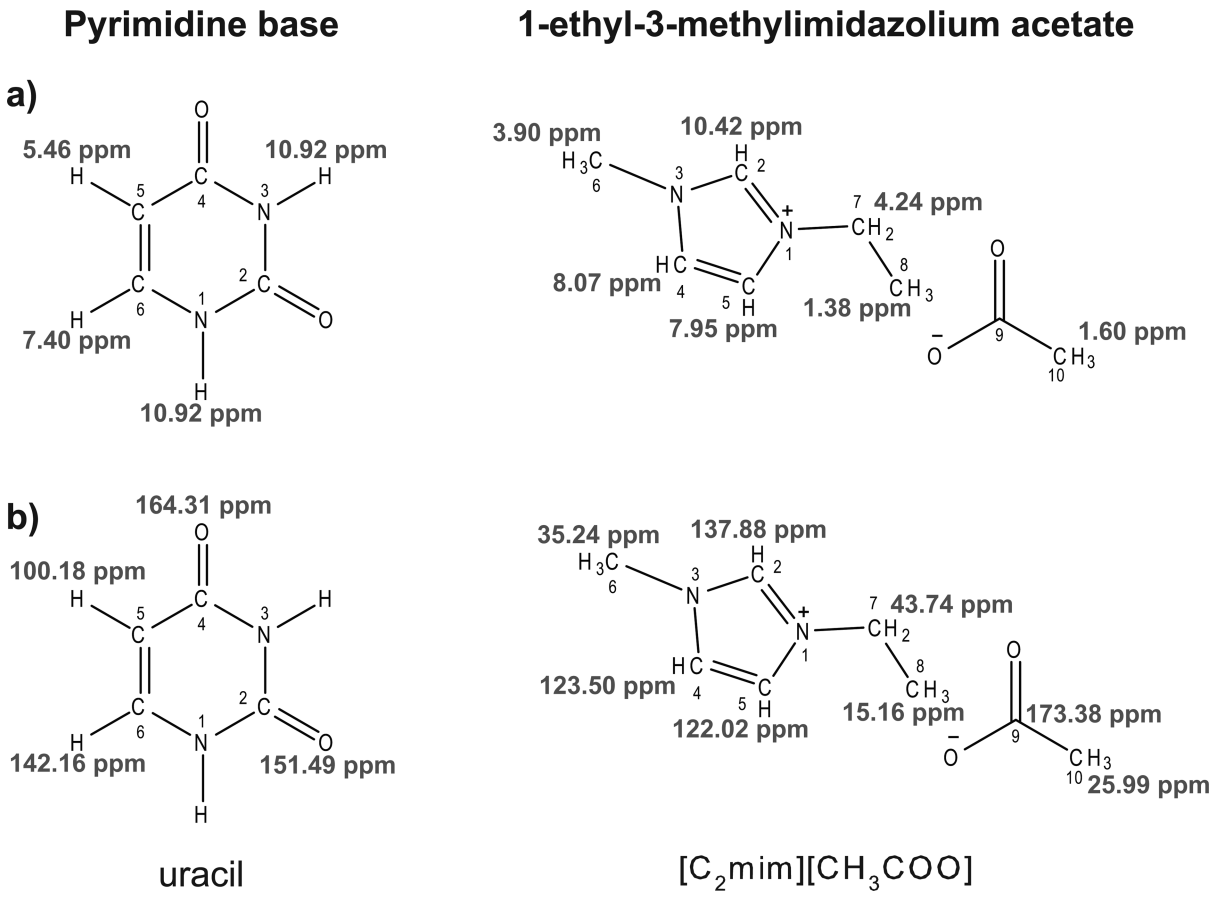

Figure 1. Proton (a) and carbon (b) chemical shifts in DMSO-d_6 and numbering system for the pyrimidine nucleic acid base uracil and the ionic liquid 1-ethyl-3-methylimidazolium acetate ([C_2mim][CH_3COO]).

recognized, mainly in those derived from the 1,3-dialkylimidazolium cation.[18−20] It is well-established that the structures of these ILs should not be considered as statistical aggregates of anions and cations but instead as 3-D networks of anions and cations, interacting via hydrogen bonds. Also, some recent experimental and theoretical studies focused on the relationship between hydrogen-bonding and the occurrence of structural changes in ILs induced by molecular solutes.[21−23]

The IL 1-ethyl-3-methylimidazolium acetate ([C_2mim][CH_3COO]) (cf. Figure 1, which also gives the numbering system for the IL) has been increasingly recognized as a promising solvent and can be regarded as an enzyme-friendly cosolvent for biocatalysis[24] as well as a good solvent for biomacromolecules such as cellulose[25,26] and suberin,[10] DNA, proteins,[27] small solutes such as carbohydrates,[28] and nucleic acid bases[29,30] and has significant ability for sour gas sequestration.[31] The small and polar $[CH_3COO]^-$ anion has the capacity to form hydrogen bonds with the bulky $[C_2mim]^+$ cation, as identified by Dhumal and coworkers[19] using quantum chemistry calculations and spectroscopic techniques. The referred study concluded that the lowest energy conformers exhibit strong C2−H···O interionic interactions compared with other conformers. The bidentate carboxylate group is responsible for this strong directionality of the interactions.

Nucleic acid bases, nitrogenous heterocyclic nucleic acids that form the structural units of DNA and RNA, are ubiquitous in nature and are of paramount importance as biochemical compounds. Their chemistry influences different synthetic pathways as well as enzyme systems and dictates the structure and properties of living cells and organisms. The interest in nucleobases solution chemistry[29,30,32,33] is growing as the knowledge of its biochemical importance and applications is becoming better known.[34−36] The practical importance of dissolving nucleobases in ILs resides on the relevance of the solutes. For example, uracil is an interesting molecule due to not only its biological significance but also its numerous therapeutic effects and applications in industrial chemistry and agriculture.[37]

In our previous studies,[29,30] 1,3-dialkylimidazolium acetate ILs have been found to be excellent solubilizers of pyrimidine (uracil and thymine) and purine (adenine) nucleic acid bases. It was possible to dissolve up to 30 wt % of uracil in [C_2mim][CH_3COO], whereas its water solubility is circa 0.3 wt %,[38] a one-hundred-fold increase. In one of those studies,[29] a preliminary analysis of the dissolution mechanism of nucleobases in 1,3-dialkylimidazolium acetate ILs, based on NMR spectroscopy, revealed that the dissolution proceeds through the partial disruption of the IL interionic hydrogen-bonded network, leading to the formation of new intermolecular hydrogen bonds. Moreover, it was verified that hydrogen-bonding between nucleobases and the acetate anion is the major driving force for nucleic acid base dissolution into 1,3-dialkylimidazolium acetate ILs. However, hydrogen-bonding between nucleobases and the imidazolium cation also participates in the dissolution process, and such effect should not be neglected. Simplified model systems (primary solvation sites) have been proposed, providing some information concerning the interactions involved in the solvation process.

dx.doi.org/10.1021/jp400749j | J. Phys. Chem. B 2013, 117, 4109−4120

Here we use ^{1}H and ^{13}C NMR spectroscopy techniques to analyze in detail the solvation of uracil in $[C_2mim][CH_3COO]$, focusing on both ions of the IL and the uracil molecule. The investigation is based on the monitoring of the hydrogen-bonding behavior of the dissolution mechanism over the entire solubility concentration range. Moreover, density functional theory (DFT) calculations have been used to validate and further describe the system. Additionally, 2D nuclear Overhauser effect spectroscopy (NOESY) NMR experiments have been implemented to probe close contacts between solute and IL ions. These analyses will be able to corroborate the previously proposed primary interactions model (solvation sites) as a simple model to address the issue of the dissolution of uracil in the IL 1-ethyl-3-methylimidazolium acetate.

2. EXPERIMENTAL SECTION

2.1. Chemicals. Uracil (2,4-dihydroxypyrimidine, ≥99%) was purchased from Sigma-Aldrich (Sheinheim, Germany) and was used without further purification. The IL $[C_2mim][CH_3COO]$ (1-ethyl-3-methylimidazolium acetate, assay >95% mass fraction, halides (ion chromatography, IC) < 1%, acetate (IC) > 95%, water (Karl Fischer titration, KF) < 5000 ppm, lot G00101.4) was supplied by IoLiTec. The IL was dried in vacuo (3×10^{-2} Torr) with vigorous stirring at 318 K for at least 4 days and was kept in vacuum until used. The water content, determined by KF, was <1000 ppm (0.1 water mass %). No further purification of the IL was carried out. The purity of the IL was checked by ^{1}H NMR analysis using dimethylsulfoxide-d_6 (DMSO-d_6) as a solvent. (See the spectrum in the Supporting Information.) The total peak integral in the ^{1}H NMR spectrum determined the nominal purities of the IL on a molar basis. The attested NMR molar fraction purity was 99.4%. The structures of uracil and $[C_2mim][CH_3COO]$ are shown in Figure 1.

2.2. NMR Sample Preparation. To analyze the changes in the ^{1}H and ^{13}C chemical shifts of the IL with increasing uracil concentration, we prepared samples gravimetrically using an analytical high-precision balance with an uncertainty of $\pm 10^{-5}$ g by adding different amounts of uracil into solutions of 0.25 g IL and 0.25 g DMSO-d_6. Upon complete dissolution, the samples were transferred to 5 mm NMR tubes containing the same amount of DMSO-d_6. Similarly, to analyze the effect in the ^{1}H and ^{13}C chemical shifts of uracil with increasing IL concentration, samples were prepared by adding different quantities of IL into solutions of 0.075 g uracil and 1.425 g DMSO-d_6. Some of these samples were also used to acquire $^{1}H-^{1}H$ NOESY spectra. DMSO-d_6 was used as an internal reference and for field-frequency lock.

2.3. NMR Measurements. The ^{1}H and ^{13}C NMR spectra of all samples were carried out on a Bruker AVANCE 400 spectrometer operated at room temperature with 16 and 500 scans, respectively. NOESY NMR experiments were obtained on a Bruker AVANCE 400 spectrometer using standard library sequences with mixing times of 50, 300, and 600 ms at room temperature. All spectra were acquired using DMSO-d_6 for field-frequency lock and NMR internal standard. Samples were prepared as outlined above.

2.4. Quantum Chemical Calculations. The geometries of the uracil−$[C_2mim][CH_3COO]$ complexes were fully optimized using DFT calculations at the B3LYP exchange correlation functional and 6-311+G(d,p) basis sets. The suitability of DFT procedures in the study of weak hydrogen-bonding interactions has been discussed in several studies.[39−41] For example, the work of Del Bene et al.[42] concluded that in most cases B3LYP and MP2 results on hydrogen bonded systems are comparable. The B3LYP exchange correlation functional reproduces the hydrogen-bonded structure and IR frequency shifts quite well.[43−45] It should be stressed that the purpose of these calculations is not a quantitative reproduction of various thermochemical and spectroscopic parameters that certainly require larger basis sets and that our interest lies rather in their quantitative trend and the underlying correlation between them. All quantum chemical calculations were performed using the Gaussian 09 program package.[46] The optimized geometries were recognized as local minima with no imaginary frequency and have been obtained using a very tight criterion of convergence. The interaction energy has been evaluated and corrected from the basis set superposition error (BSSE) according to the site−site function (SSFC) scheme.[47−50] Geometry optimizations were performed without any constraints.

3. RESULTS AND DISCUSSION

The main objective of the present study is to model the uracil−$[C_2mim][CH_3COO]$ solvation interactions as a way to understand the primary factors contributing to uracil solubility in the IL and consequently estimate the hydrogen-bonding contribution to the previously proposed dissolution mechanism.[29]

On the basis of the NMR studies discussed in detail elsewhere,[29] we can conclude that the hydrogen bonding between the hydrogen atoms of the N1−H or N3−H groups in uracil and the relatively small acetate anion of the IL is the main driving force for nucleic acid base dissolution into 1-ethyl-3-methylimidazolium acetate IL. However, the hydrogen-bonding between the oxygen atoms of the carbonyl groups in uracil and the ring hydrogen atoms of the imidazolium cation, especially the H2 hydrogen atom, cannot be neglected. Additionally, in that work,[29] we have complemented our NMR results with other experimental and theoretical results, such as the study from Leist et al.,[51] showing that hydrogen-bonding wins over π stacking in the binary intermolecular interaction of fluorobenzene with nucleobase, which gave us the confidence to generalize the hydrogen-bonding concept and suggest that the imidazolium cation can also have a direct role in the dissolution process. Moreover, those results[29] also have shown that the dissolution of uracil in the IL can be understood as a gradual disruption of the IL interionic hydrogen-bonded network, leading to the formation of new intermolecular hydrogen bonds.

Toward a better understanding of the specific roles of the cationic and anionic components of $[C_2mim][CH_3COO]$ on the uracil dissolution process and in order to elucidate the uncertainty concerning the role of hydrogen-bonding in the imimidazolium cation−uracil interactions, we have carried out a detailed NMR analysis in an extended concentration range, focusing on both ions of the IL and the uracil molecule.

Additionally, a detailed analysis of the distance and angular distribution of anions, cations, and uracil molecules has been addressed using chemical calculations by the use of DFT methods. Despite the ongoing debate concerning the specific nature of hydrogen bonds, it is generally accepted that the interaction is 90% electrostatic. Concerning the detection of hydrogen bonds in atomistic simulations or crystal structures, some standard definitions are often employed based on purely geometric criteria. As an example, a typical X−H···Y interaction

dx.doi.org/10.1021/jp400749j | J. Phys. Chem. B 2013, 117, 4109−4120

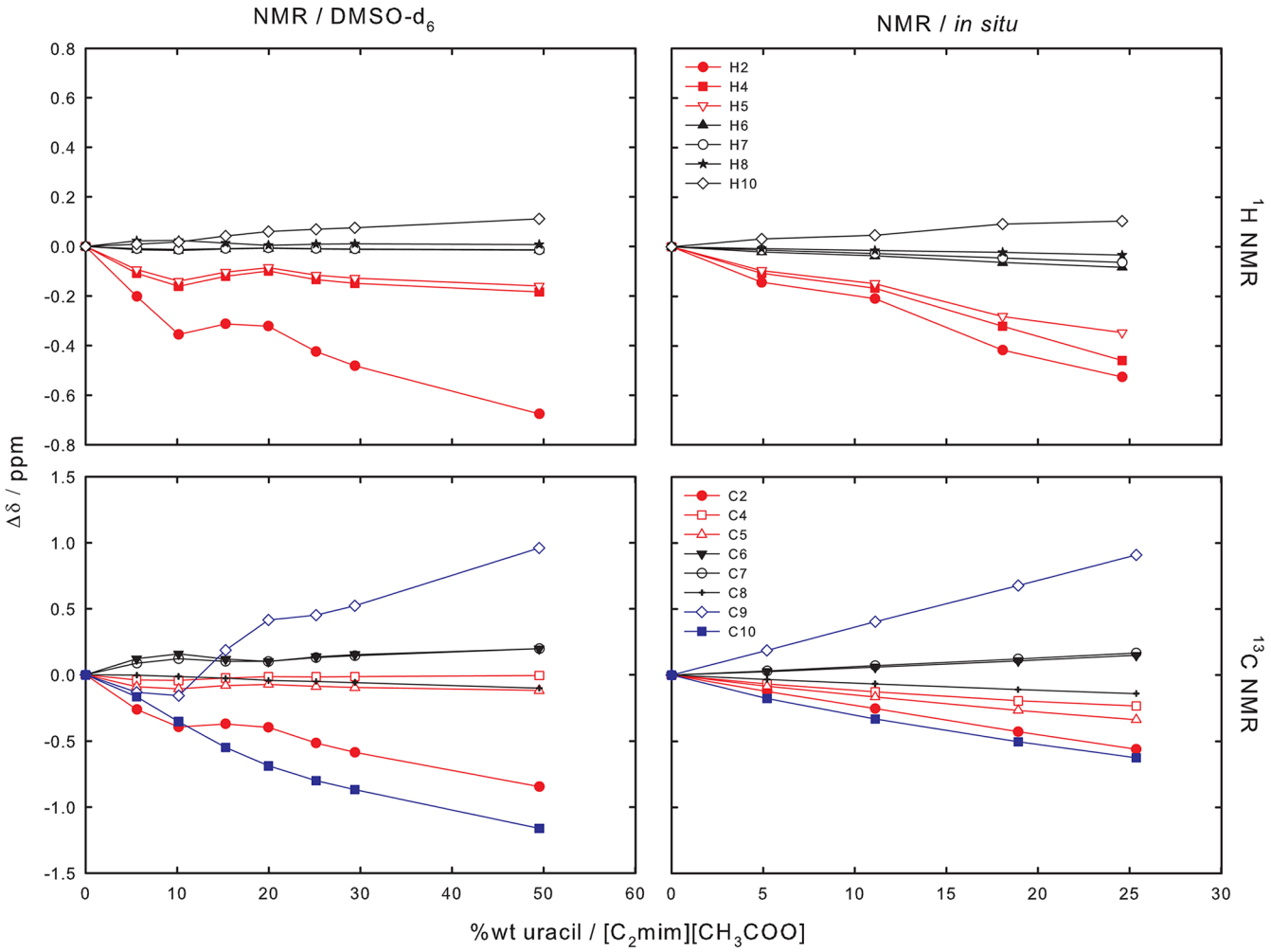

Figure 2. Trend of the chemical shift difference of protons in ^{1}H NMR and carbons in ^{13}C NMR of $[C_2mim][CH_3COO]$ with increasing nucleobase concentration ($\Delta\delta = \delta - \delta_{neat}$). The ring protons in the imidazolium cation (highlighted red), especially H2, show a marked upfield shift. The anion carbons (highlighted blue) show distinct behavior: the signal of the carboxyl (C9) moves downfield significantly, and the methyl carbon (C10) presents an upfield change. Both sets of results for the studies in DMSO-d_6 solution and in situ are depicted.

may be considered to be a hydrogen bond if $r_{H\cdots Y} < 2.5$ Å[52] and $\theta_{XH\cdots Y} > 150°$. The potential hydrogen bonds analyzed in the following discussion are N−H···O and C−H···O. There are many different angles and distances that can be measured and used to identify the hydrogen bond. For Baker and Hubbard,[53] a N−H···O hydrogen bond is assigned when the angle $\theta_{NH\cdots O} > 120°$ and the distance $r_{H\cdots O} < 2.5$ Å. Although, in a typical hydrogen-bonding environment the X−H···Y hydrogen bond angle tends toward 180° and should preferably be above 110° (as stated in the IUPAC recommendations 2011 for the definition of the hydrogen bond[54]).

Finally, ^{1}H−^{1}H NOESY NMR data have also been acquired to probe the close contacts between uracil and IL cation and validate the direct role of the hydrogen bonding between the $[C_2mim]^+$ cation and the uracil molecule during the dissolution.

3.1. ^{1}H NMR and ^{13}C NMR Chemical Shift Analysis. In the discussion of our previous work[29] it was clearly shown that the formation of hydrogen bonds between uracil and the IL ions affects the chemical shifts of the involved hydrogen atoms as well as the chemical shifts of the carbon atoms around the involved groups of the IL. Accordingly, the effect of uracil concentration on such chemical shift differences ($\Delta\delta = \delta - \delta_{neat}$) is an unequivocal method to track the suggested hydrogen-bonding patterns. In fact, such method, the detection and analysis of the chemical shift perturbation ($\Delta\delta$) using ^{1}H and ^{13}C NMR spectra of solution with different concentrations, has been extensively applied to prove the existence of hydrogen-bond interactions.[55−58]

The previous NMR-based investigations[29] of the uracil−$[C_2mim][CH_3COO]$ interactions were carried out in the absence of cosolvent, and the study of $\Delta\delta$ values was accomplished using external references. With this in situ approach, the contact between the deuterated solvent and the IL and the nucleic acid base was avoided, preventing possible interactions that could interfere with those occurring between uracil and the IL.

To expand the scope of the previous investigations,[29] we extended the NMR study to encompass the effect of the IL on the proton and carbon chemical shifts of the uracil molecule, thus identifying experimentally the uracil sites participating in the nucleobase−IL interactions. This means that these measurements must be carry out in the presence of a cosolvent, namely using DMSO-d_6 solutions. One may wonder if the addition of DMSO-d_6 can interfere with the interactions occurring between uracil and $[C_2mim][CH_3COO]$ and hinder

dx.doi.org/10.1021/jp400749j | J. Phys. Chem. B 2013, 117, 4109−4120

the dissolving capability of the IL for the nucleic acid base. To answer this question, we have studied the effect of uracil concentration on the ^{1}H and ^{13}C chemical shifts of the IL in DMSO-d_6 solutions. These results are summarized in Figure 2, where we can observe that they present a similar trend to those obtain in situ[29] (also depicted in the Figure), indicating that the mechanism model obtained in DMSO-d_6 is also suitable for the real system. In fact, it has been reported that the addition of DMSO-d_6 as a cosolvent made no impact on the chemical shifts of polysaccharides.[59−61] Also, Remsig and coworkers[62] suggested that interactions between the anions and cations in ILs were not affected but slightly enhanced as the DMSO content increased. Moreover, although in some cases DMSO can be considered to be a potential hydrogen-bond acceptor, its hydrogen-bond acceptor ability (Kamlet−Taft β parameter = 0.69[63]) is much lower than that of [C_2mim][CH_3COO] (β = 1.09;[63] 0.95[64]). Besides, the hydrogen-bond donor ability of [Cmim][CH_3COO] (Kamlet−Taft α parameter = 0.5;[63] 0.4[64]) is much higher than that of DMSO (α = 0), which is not a hydrogen-bond donor. Furthermore, uracil, like the other nucleic acid bases, has a great versatility in the formation of hydrogen bond complexes because of the presence of several hydrogen-bond donor and acceptor groups. Uracil has two adjacent *cis*-amide groups, which originate four double hydrogen-bonding sites, each with a hydrogen-bond donor and acceptor, as depicted in Figure 3. The designation of the

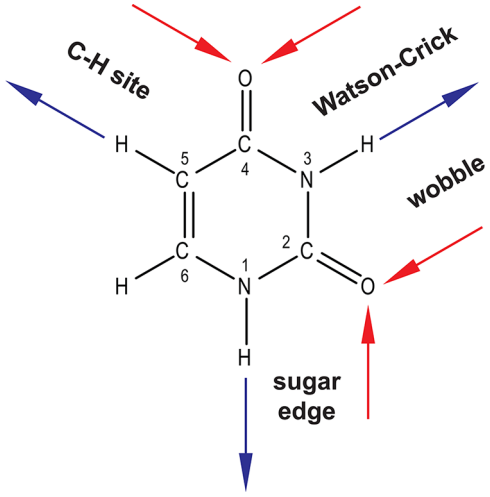

Figure 3. Structure and numbering of the pyrimidine nucleic acid base uracil. The hydrogen-bond donor (blue) and acceptor (red) sites are highlighted by arrows, and the four possible hydrogen-binding sites are labeled.

four binding sites is also illustrated in Figure 3 as follows: the N1−H donor together with the C2═O acceptor hydrogen-bonding sites are denoted as the "sugar edge";[65] the N3−H hydrogen-bonding donor and the C2═O hydrogen-bond acceptor sites form the so-called "wobble" binding site;[66] the N3−H hydrogen-bonding donor and C4═O hydrogen-bonding acceptor sites form the Watson−Crick site;[67] the fourth double hydrogen-bonding site denoted the "C−H site"[68] is formed by the C5−H (weak hydrogen-bonding donor) and C4═O groups. The interaction energies of the above-mentioned binding sites will depend not only on the basicity of the acceptor groups but also on the acidity of the donor groups. The basicity of uracil has been addressed in several works,[69−71] and it has been suggested that both carbonyl groups are comparable in their acceptor strength. Relative to the acidity of uracil, it must be stressed here that the intrinsic acidity is in part responsible for the natural selection of molecules acting as principal biological hydrogen donors. This property may be partially responsible for the natural selection of these biological molecules[72,73] and must also be the leading factor for the nucleic acid bases. The acidity of uracil is reflected by its pK_a in water (9.5),[74,75] which is very similar to that of 4-chlorophenol (9.4). Accordingly, the addition of DMSO-d_6 as a cosolvent has no impact on the experimental results, as depicted in Figure 2.

The experimental identification of the uracil sites involved in the nucleobase−IL interactions has been attained by the analysis of the $\Delta\delta$ values using ^{1}H and ^{13}C NMR spectra of uracil/DMSO-d_6 solutions with different IL concentrations. The ^{1}H and ^{13}C NMR spectra of uracil in DMSO-d_6 are shown in Figures S1 and S2 of the Supporting Information. The assignment has been done accordingly with the literature.[76] The effect of [C_2mim][CH_3COO] concentration on the proton and carbon chemical shifts is illustrated in Figures 4 and 5 to achieve a better understanding on the uracil sites involved in the interactions with [C_2mim][CH_3COO]. When [C_2mim][CH_3COO] is added to uracil/DMSO-d_6 solution, a significant broadening of the peak assigned to the protons of the hydrogen-bonding donor sites N1−H and N3−H is observed, as depicted in Figure 4. The main reason for the significant broadening of these proton resonances (N1−H and N3−H) is the interaction of these protons with the oxygen atom of the IL [CH_3COO]$^-$ anion, as clearly indicated by the ^{13}C $\Delta\delta$ values of [C_2mim][CH_3COO] (significant downfield shift of the carbonyl C9 carbon) as the uracil concentration increases in the [C_2mim][CH_3COO]/DMSO-d_6 solution and in the in situ NMR studies, as depicted in Figure 2. The significant downfield shift of the carbon resonances of both hydrogen-bonding acceptor sites (C2═O and C4═O) of uracil as the [C_2mim][CH_3COO] concentration increases, as presented in Figure 5, indicates that the oxygen atoms of the carbonyl groups in uracil form hydrogen bonds with the hydrogen atoms of the IL imidazolium ring. Accordingly, as the uracil concentration increases in the [C_2mim][CH_3COO]/DMSO-d_6 solution and in the in situ NMR studies, only the ring protons in the imidazolium cation, especially H2, show a marked upfield shift, whereas the other protons of the IL show negligible change (cf. Figure 2). These indicate that only the aromatic hydrogens atoms of the imidazolium cation (H2, H4, and H5), especially H2, form hydrogen bonds with the uracil carbonyl groups oxygens. Indeed, it has been reported that because the aromatic hydrogens atoms are the most acidic hydrogens in the IL (especially H2) they can form hydrogen bonds with oxygen atoms in acetone,[77] alcohols,[78] water,[79,80] and so on. Therefore, it is reasonable to assume that the upfield shift of the imidazolium ring protons is due to the disruption of the interionic hydrogen bond between the IL cation and anion and the formation of weaker ones involving the IL cation and the nucleobase hydrogen-bond acceptor sites. The effect of uracil concentration on the ^{1}H and ^{13}C NMR of [C_2mim]-[CH_3COO] spectra in DMSO-d_6 and in situ is illustrated in Figure S5 of the Supporting Information.

Both sets of NMR data, the effect of uracil concentration on the proton and carbon chemical shifts of the IL depicted in Figure 2 (see also Figure S5 of the Supporting Information) and effect of the IL concentration on the proton and carbon chemical shifts of uracil presented in Figures 4 and 5,

dx.doi.org/10.1021/jp400749j | J. Phys. Chem. B 2013, 117, 4109−4120

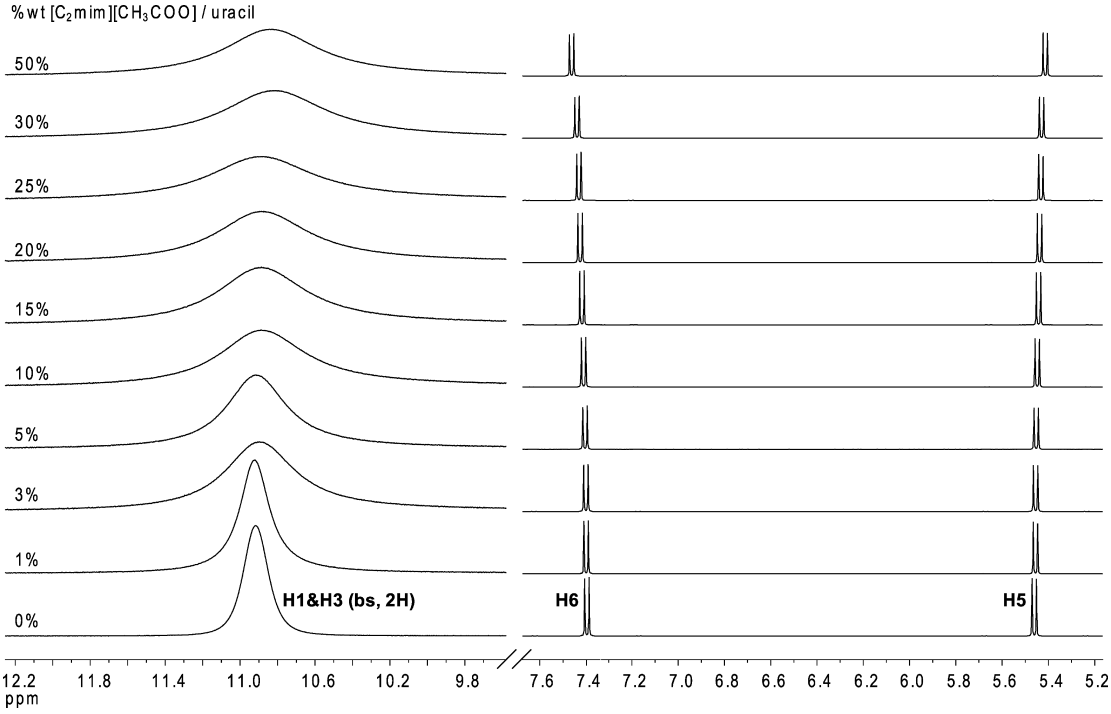

Figure 4. Effect of $[C_2mim][CH_3COO]$ concentration on the ^1H NMR of uracil spectra in DMSO-d_6. Only the peak assigned to the protons of the hydrogen-bonding donor sites (N1−H and N3−H) presents a significant broadening. The protons of both C−H5 and C−H6 groups show negligible change. The bottom spectrum is the neat uracil in DMSO-d_6.

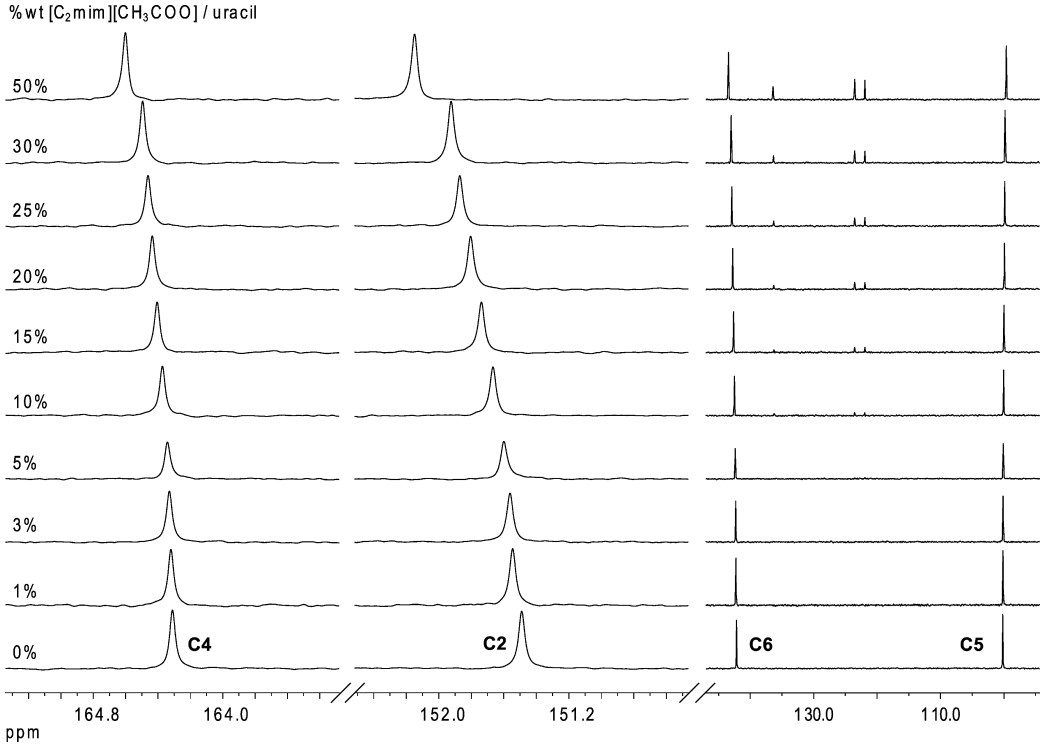

Figure 5. Effect of $[C_2mim][CH_3COO]$ concentration on the ^{13}C NMR of uracil spectra in DMSO-d_6. The signal of both carbonyl groups (C2═O and C4═O), the hydrogen-bonding acceptor sites, moves downfield significantly. The bottom spectrum is the neat uracil in DMSO-d_6.

corroborate the previously proposed dissolution mechanism.[29] A schematic view of the dissolution process of uracil in $[C_2mim][CH_3COO]$ is summarized in Figure 6, where hydrogen-bonding between the hydrogen atoms of N1−H and N3−H groups of uracil and the $[CH_3COO]^-$ anion and between the most acidic hydrogen atom (H2) of the imidazolium cation and the oxygen atoms of the carbonyl groups of uracil is controlling the solvation process. Also, for disclosing the dissolution process, the saturation molar ratio of uracil−$[C_2mim][CH_3COO]$, obtained using the solubility

dx.doi.org/10.1021/jp400749j | J. Phys. Chem. B 2013, 117, 4109−4120

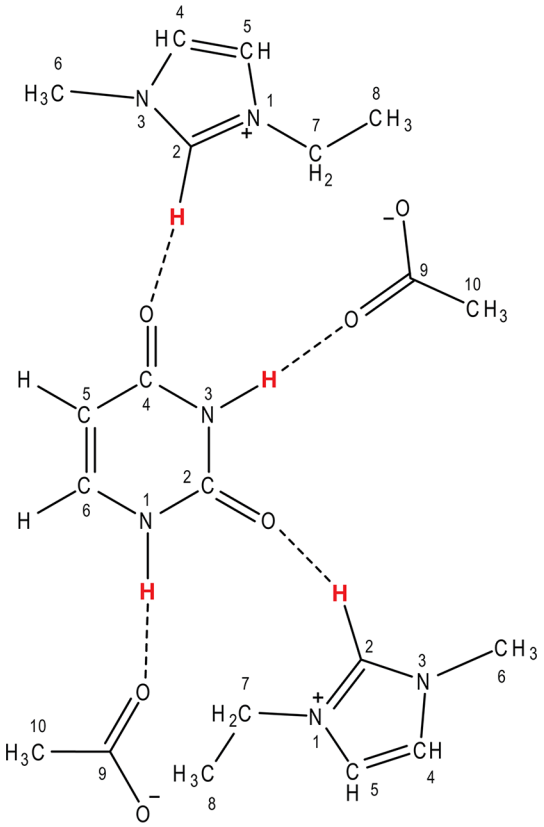

Figure 6. Schematic illustration of the primary solvation sites of uracil with $[C_2mim][CH_3COO]$. Hydrogen-bonding between the hydrogen atoms of N1−H and N3−H groups of uracil and the $[CH_3COO]^-$ anion and between the most acidic hydrogen atom (H2) of the $[C_2mim]^+$ cation and the oxygen atoms of the carbonyl groups of uracil causes the solvation. The H2 hydrogen atom of the imidazolium ring and the hydrogen atoms of the hydrogen-bonding donor sites of uracil are highlighted in red to point out the potential through-space interactions to be ascertained by NOESY NMR experiments.

value[29,30] of uracil in 1-ethyl-3-methylimidazolium acetate IL at 298 K, have been used. The stoichiometric ratio of uracil to $[C_2mim][CH_3COO]$ is 1:2. It is important to remark that the analysis of the proton and the carbon chemical shift deviations depicted throughout the paper was plotted to illustrate a specific trend, that is, an analysis to better summarize the effect of uracil or $[C_2mim][CH_3COO]$ concentration in the "shielding" or "deshielding" effect on a nucleous of a specific atom in a chemical group of the IL or uracil, respectively. The ^1H and ^{13}C NMR spectra of neat $[C_2mim][CH_3COO]$ in DMSO-d_6 are given in the Supporting Information (Figures S3 and S4). The assignment was performed with 2D COSY and HSQC experiments and is in accordance with the literature.[30,81,82]

A final comment concerning the broadening of the N1−H and N3−H protons of uracil (cf. Figure 4) is necessary once the broadening of these signals might also indicate increased mobility of the protons due to proton transfer to the IL acetate anion, which also explains the downfield shift of the carbonyl C9 carbon of the acetate anion (cf. Figure 2 and Figure S5 in the Supporting Information). If the proton transferring to the acetate anion occurs, then acetic acid will be formed. The possible existence of acetic acid in the binary mixture uracil + $[C_2mim][CH_3COO]$ was checked during the experimental work by pH measurements of the samples studied at 298 K. From neat IL, throughout binary uracil + $[C_2mim][CH_3COO]$ solutions near uracil saturation limit (30 wt % of uracil in $[C_2mim][CH_3COO]$) the pH value remained constant, which clearly indicates that the formation of acetic acid did not occur, and thus the transferring of the N1−H and N3−H protons to the acetate anion did not take place. Additionally, in a previous work,[8] concerning a protic system with the same IL ($[C_2mim][CH_3COO]$), we checked the possible existence of acetic acid in the binary mixture $[C_2mim][CH_3COO]$ + $[NH_4][SCN]$ at 298 K and atmospheric pressure (the same experimental conditions of the present work) up to 30 days. ATR-FTIR spectroscopy was quantitatively used to determine the acetic acid content. The amount of acetic acid found (<2 wt %) was small and considered to be negligible. If the N1−H and N3−H proton transferring to the acetate anion would occur in our mixtures, then we should expect that the spectrum is a composite one resulting from the addition of the spectrum of uracil and of the deprotonated species. In that case, we should detect secondary lines of lesser intensity in the vicinity of each main resonance lines of uracil, corresponding to the deprotonated species. Similar to the observations of Besnard et al.[83] in the study of the solvation of CO_2 in $[C_4mim][CH_3COO]$, where they came to the conclusion that CO_2 reacts with the imidazolium cation, leading to the carboxylation of the imidazolium ring and concomitantly to the formation of acetic acid. Secondary resonance lines were not observed on the ^1H and ^{13}C NMR spectra depicted in Figures 4 and 5, respectively. Also, if proton transferring to the acetate anion and concomitant formation of acetic acid occurs, then a resonance line should be detected in the uracil + $[C_2mim][CH_3COO]$ mixtures and assigned to the COOH group of the acid molecule interacting with "free" oxygen atom of the IL $[CH_3COO]^-$ anion. Mixtures of acetic acid with polar solvents are well studied,[84−87] showing that the population of monomers and linear forms that may form complexes with the solvent increases as the population of cyclic dimers decreases. This situation also occurs for acetic acid diluted in the IL $[C_2mim][CH_3COO]$. From the work of Dhumal et al.,[19] where it was demonstrated that the most probable short-ranged local structure of $[C_2mim][CH_3COO]$ consists of anions in which an oxygen atom of the carboxylate group interacts in a monodentate configuration with a proton of the imidazolium ring (mainly with the C2−H proton), leaving the remaining oxygen atom available for other interactions, we may infer that the COOH group of monomers and dimers of acetic acid molecule interacts through hydrogen bond with the available oxygen atom of the IL $[CH_3COO]^-$ anion, whereas the other oxygen atom is hydrogen-bonded to the $[C_2mim]^+$ ring. A resonance line associated with this interaction is not observed in the ^1H NMR spectra of uracil + $[C_2mim][CH_3COO]$ mixtures in DMSO-d_6 and in situ, which depicts the effect of uracil concentration on the ^1H spectra of $[C_2mim][CH_3COO]$ (Figure S5 of Supporting Information and the ^1H NMR spectra in our previous work addressing the solvation of nucleobases in 1,3-dialkylimidazolium acetate ILs[29]). Such an interaction is observed and attested in the study of CO_2 + $[C_4mim][CH_3COO]$ mixtures.[83] Grounded in the ^1H and ^{13}C NMR studies and the lack of observation of the secondary resonance lines and the resonance line associated with the COOH−$[CH_3COO]^-$ interaction and in the pH measurements, we can conclude that the N1−H and N3−H proton transferring to the acetate anion and concomitant formation of acetic acid do not occur.

dx.doi.org/10.1021/jp400749j | J. Phys. Chem. B 2013, 117, 4109−4120

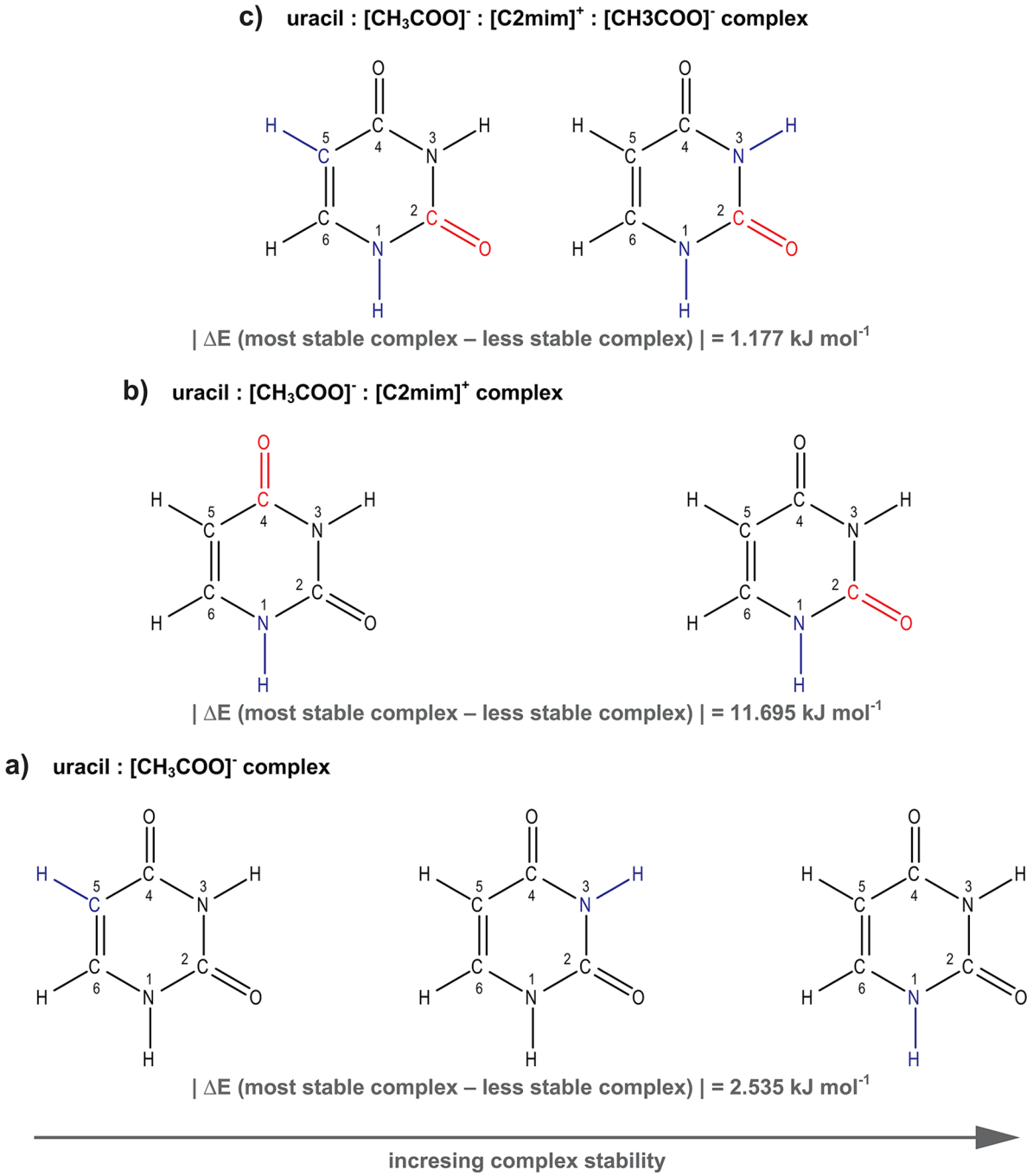

Figure 7. Analyses of the complexes (a) uracil–$[CH_3COO]^-$, (b) uracil–$[CH_3COO]^-$–$[C_2mim]^+$ (1:1 uracil–$[C_2mim][CH_3COO]$), and (c) uracil–$[CH_3COO]^-$–$[C_2mim]^+$–$[CH_3COO]^-$ based on the four hydrogen-binding sites labeled in Figure 3. The uracil hydrogen-bond donor and acceptor sites are highlighted in blue when interacting with the IL $[CH_3COO]^-$ anion and highlighted in red when interacting with the H2 hydrogen atom (most acidic) of the $[C_2mim]^+$ cation, respectively. As indicated, for each set of data the complexes are depicted in increasing complex stability order (i.e., decreasing interaction energy).

3.2. Quantum Chemical Calculations of the Interactions between Uracil and $[C_2mim][CH_3COO]$. The use of methods such as DFT, where the electronic structure of the molecules is explicitly considered, to accurately describe the interactions presents in the system uracil–$[C_2mim]$-$[CH_3COO]$ seems to be an obvious choice in the present context. To calculate the preferred hydrogen-bonding interactions between uracil and $[C_2mim][CH_3COO]$, we have selected all of the possible hydrogen-binding sites in uracil molecule (depicted in Figure 3) to perform DFT calculations. The optimized geometries of the most stable complexes are shown in Figure 8. The sum of the van der Waals atomic radii of H and O atoms, 2.5 Å, is used as a criterion for hydrogen bonding.[52] Hydrogen bonds are denoted by dashed lines, and the corresponding H···O distances and X–H···O angles are labeled in the Figure.

Taking into account the four possible uracil hydrogen-binding sites (labeled in Figure 3) and the experimental ^1H and ^{13}C NMR results, showing that the acetate anion forms stronger hydrogen bonds with the hydrogen atoms of the hydrogen-

dx.doi.org/10.1021/jp400749j | J. Phys. Chem. B 2013, 117, 4109–4120

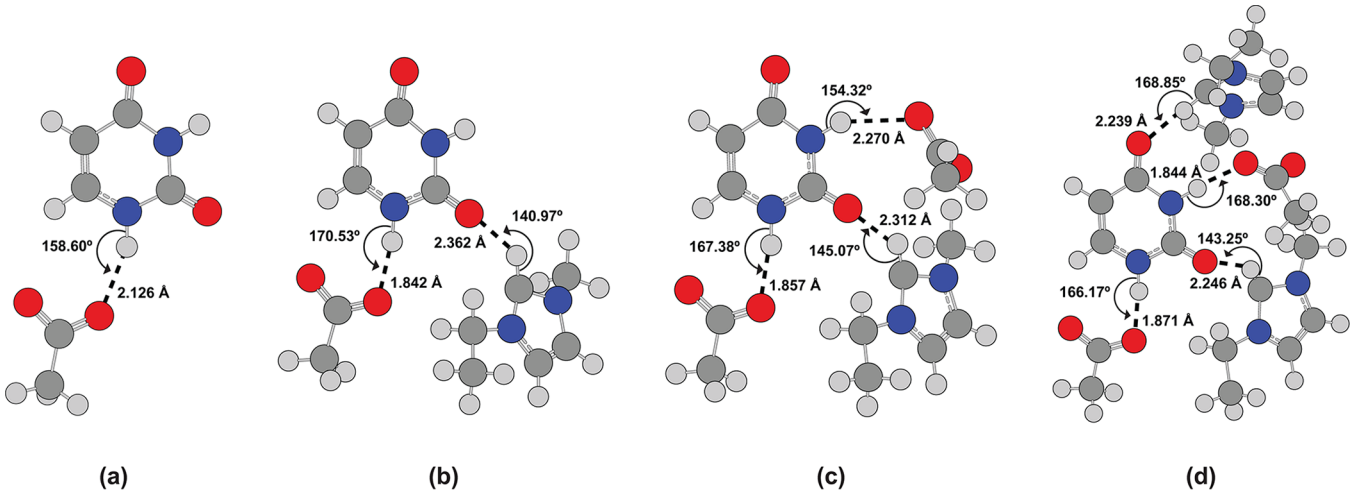

Figure 8. Optimized geometries of the most stable complexes of the types (a) uracil−$[CH_3COO]^-$, (b) uracil−$[CH_3COO]^-$−$[C_2mim]^+$ (1:1 uracil−$[C_2mim][CH_3COO]$), (c) uracil−$[CH_3COO]^-$−$[C_2mim]^+$−$[CH_3COO]^-$, and (d) uracil−$[CH_3COO]^-$−$[C_2mim]^+$−$[CH_3COO]^-$−$[C_2mim]^+$ (1:2 uracil−$[C_2mim][CH_3COO]$). Hydrogen bonds are denoted by dashed lines. The values of the corresponding H···O distances as well as the N−H···O and C−H···O angles are shown.

bond donor sites of uracil than the hydrogen atoms of the imidazolium cation,[29] the strategy for the quantum chemical calculations was established as follows (Figure 7): first, the analysis of the interaction between one $[CH_3COO]^-$ anion and the three possible hydrogen-donor sites of uracil (highlighted in blue in Figure 3) was considered; then, based on the most stable uracil−$[CH_3COO]^-$ complex, the analysis was extended to the interaction of uracil with both one $[CH_3COO]^-$ anion and one $[C_2mim]^+$ cation; the most stable 1:1 uracil−$[C_2mim][CH_3COO]$ complex (uracil−$[CH_3COO]^-$−$[C_2mim]^+$ complex) was then used as the starting point for the inclusion of a second $[CH_3COO]^-$ anion. Finally, the analysis was extended to obtain the most stable 1:2 uracil−$[C_2mim][CH_3COO]$ complex.

The results of the quantum chemical calculations of the complexes uracil−$[CH_3COO]^-$ (Figure 7a), modeling the interactions between the IL acetate anion and uracil, indicates, as expected, that the most stable interactions involve the uracil hydrogen-donor sites N1−H and N3−H. In the most stable uracil−$[CH_3COO]^-$ complex (Figure 8a), the uracil hydrogen atom of the N1−H group hydrogen-bonds with the $[CH_3COO]^-$ anion with a H···O distance of 2.126 Å and a N−H···O angle of 158.60°.

To understand how uracil interacts with both the anion and the cation simultaneously, we performed the DFT evaluation of 1:1 uracil−$[C_2mim][CH_3COO]$ complexes (uracil−$[CH_3COO]^-$−$[C_2mim]^+$ complex). The results are depicted in Figure 7b. As can be seen in Figure 8c, the most stable 1:1 uracil−$[C_2mim][CH_3COO]$ complex presents hydrogen-bonding interactions between the hydrogen atom of the N1−H uracil group and the $[CH_3COO]^-$ anion with a H···O distance of 1.842 Å and a N−H···O angle of 170.53° and between the H2 hydrogen of the imidazolium ring (most acidic) and the oxygen atom of the uracil C2═O group with a H···O distance of 2.362 Å and a C−H···O angle of 140.97°. This result shows that the C2═O hydrogen-bond acceptor site of uracil can form stable hydrogen bonds with the C2−H, consistent with the fact that the electron deficit in the imidazolium ring makes H2 the most acidic hydrogen atom on the imidazolium ring.[77−80]

Taking into account the most stable 1:1 uracil−$[C_2mim][CH_3COO]$ complex and also the fact that the uracil−$[C_2mim][CH_3COO]$ saturation molar ratio is 1:2, the interactions of uracil were extended to include a second $[CH_3COO]^-$ anion (Figure 7c). As can be seen in Figure 8), the most stable uracil−$[CH_3COO]^-$−$[C_2mim]^+$−$[CH_3COO]^-$ complex exhibits hydrogen-bonding interactions between the hydrogen atoms of the N1−H and N3−H uracil groups and the $[CH_3COO]^-$ anions with a H···O distance of 1.857 and 2.270 Å and a N−H···O angle of 167.38 and 154.32, respectively. Hydrogen bonding is also present between the most acidic hydrogen atom of the imidazolium ring cation (H2) and the oxygen atom of the uracil C2═O group with a H···O distance of 2.312 Å and a C−H···O angle of 145.07°.

Finally, following the step-by-step quantum chemical calculations depicted in Figure 7, the 1:2 uracil−$[C_2mim]$-$[CH_3COO]$ complex was considered. The optimized geometry of the 1:2 uracil−$[C_2mim][CH_3COO]$ complex is depicted in Figure 8d, revealing hydrogen-bonding interactions between the hydrogen atoms of the N1−H and N3−H uracil groups and the $[CH_3COO]^-$ anions with a H···O distance of 1.871 and 1.844 Å and a N−H···O angle of 166.17 and 168.30°, respectively. This complex also exhibits hydrogen-bonding between the H2 hydrogens of both imidazolium ring cations and the oxygen atoms of the uracil C2═O and C4═O groups with a H···O distance of 2.246 and 2.239 Å and a C−H···O angle of 143.25 and 168.85°, respectively. The uracil hydrogen-binding sites, as labeled in Figure 3, participating in the interactions with $[C_2mim][CH_3COO]$ are the so-called "sugar-edge" and Watson−Crick sites.

All of the H···O distances labeled in Figure 8 are shorter than the summation of the van der Waals radii of O and H atoms (2.5 Å). The corresponding values of N−H···O and C−H···O angles vary ranging from 154.32 to 170.53° and from 140.97 to 168.85°, respectively. These data confirm the efficient hydrogen bonds between the uracil hydrogen-bond donor and acceptor sites and the IL's anion and cation, respectively.

3.3. NOESY NMR Analysis. One of the most effective approaches to the study of molecular structure, assembly, and aggregation phenomena in ILs is nuclear Overhauser effect (NOE) spectroscopy NMR.[88] NOE data render the information of spatial proximity and dynamics of selected nuclei and therefore provide distance restrains useful to propose

dx.doi.org/10.1021/jp400749j | J. Phys. Chem. B 2013, 117, 4109−4120

aggregation geometries and assembly motives within the liquid. In the present study, the most common and important NOE experiments, ^{1}H−^{1}H homonuclear NOE, were carried out as 2-D correlations (NOESY). The key step of the NOESY pulse sequence is the so-called mixing time. The use of short mixing times[89,90] avoids the introduction of considerable spin diffusion and consequently shorter than normal internuclear H−H distances.

Considering the proposed primary solvation sites of uracil in [C_2mim][CH_3COO],[29] schematically depicted in Figure 6, where hydrogen-bonding between the hydrogen atoms of N1−H and N3−H groups of uracil and the [CH_3COO]$^-$ anion and between the most acidic hydrogen atom (H2) of the imidazolium cation and the oxygen atoms of the carbonyl groups of uracil causes the dissolution, one can clearly visualize a close contact between the most acidic hydrogen atom of the imidazolium cation (H2) and the hydrogen atoms of N1−H and N3−H groups of uracil (hydrogen atoms highlighted in red in Figure 6). Therefore, ^{1}H−^{1}H NOESY NMR spectroscopy experiments have been implemented to test the existence of such suggested close contacts.

Figure 1 gives the numbering system for the proton peaks in the 1D NMR spectrum at the top and sides of Figures 9 and 10

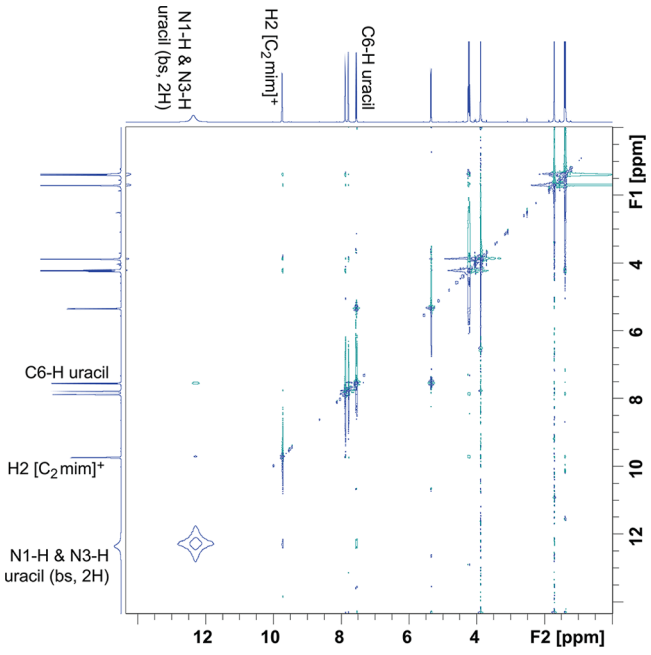

Figure 9. NOESY spectrum of 1:1 mixture of uracil−[C_2mim]-[CH_3COO] (50 wt % uracil/[C_2mim][CH_3COO]) in DMSO-d_6 at 298 K. The mixing time employed was 300 ms.

and also of Figures S6 and S7 of the Supporting Information. Additionally, the ^{1}H NMR spectrum of uracil and [C_2mim]-[CH_3COO] in DMSO-d_6 together with the assignment of the protons is depicted in Figures S1 and S3 of the Supporting Information, respectively. Figure 9 is the ^{1}H−^{1}H NOESY spectrum of 50 wt % uracil/[C_2mim][CH_3COO] in DMSO-d_6 (stoichiometric ratio of uracil to [C_2mim][CH_3COO] of 1:1) with a mixing time of 300 ms at 298 K. See the Supporting Information (Figure S6) for the ^{1}H−^{1}H NOESY spectrum of the same solution with a shorter mixing time, 50 ms. In both Figures, one observes cross peaks between the H2 imidazolium ring proton (the most acidic) and the resonance assigned to

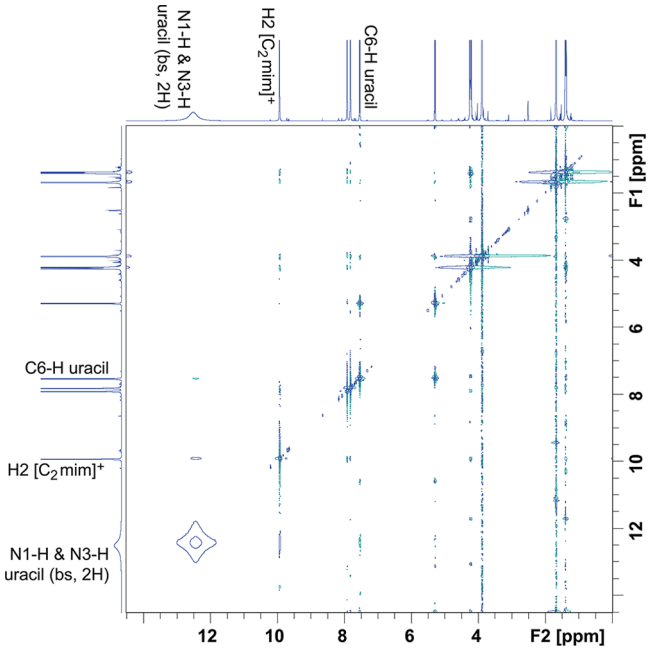

Figure 10. NOESY spectrum of 1:2 mixture of uracil−[C_2mim]-[CH_3COO] (30 wt % uracil/[C_2mim][CH_3COO]) in DMSO-d_6 at 298 K. The mixing time employed was 300 ms.

both protons of the hydrogen-bonding donor sites of uracil (bs, 2H), N1−H, and N3−H. Figure 10 depicts the ^{1}H−^{1}H NOESY spectrum of 30 wt % uracil/[C_2mim][CH_3COO] in DMSO-d_6 (stoichiometric ratio of uracil to [C_2mim]-[CH_3COO] is 1:2) with a mixing time of 300 ms at 298 K. The corresponding ^{1}H−^{1}H NOESY spectrum with a mixing time of 50 ms is presented in Figure S7 of the Supporting Information. Again, cross peaks are observed between the H2 ring proton of the imidazolium bulky cation (Figure 1) and the protons of the hydrogen-bonding donor sites N1−H and N3−H of uracil.

The analysis carried throughout the four ^{1}H−^{1}H NOESY spectra (Figures 9 and 10 and Figures S6 and S7 of the Supporting Information) probed the close contact between the protons highlighted in red in Figure 6. These findings were consisting across all mixing times employed (50−300 ms), which demonstrates that these hydrogen−hydrogen distances are not unrealistically short once the hydrogen−hydrogen distances at lengthy mixing times (300 ms) are in agreement with those at short mixing times (50 ms). These results consubstantiate the proposed primary solvation sites of uracil dissolution in the IL 1-ethyl-3-methylimidazolium acetate, schematically illustrated in Figure 6, which implies that the interactions between the H2 proton of the imidazolium ring cation (the most acidic proton) and the oxygen atoms of the hydrogen-bonding acceptor sites (C2═O and C4═O groups) of uracil do exist.

4. CONCLUSIONS

The detailed solvation mechanism of uracil in [C_2mim]-[CH_3COO] has been elucidated in the current study via the investigation of the hydrogen-bonding interactions of the IL with uracil using a combined application of ^{1}H and ^{13}C NMR spectroscopy, DFT calculations, and ^{1}H−^{1}H NOESY NMR spectroscopy. The three approaches yielded consistent results. Through the combination of the structural information with

dx.doi.org/10.1021/jp400749j | J. Phys. Chem. B 2013, 117, 4109−4120

NOESY data it has been possible to demonstrate that the primary interactions of uracil with $[C_2mim][CH_3COO]$ are associated with the $[CH_3COO]^-$ anion and that directional interactions with the $[C_2mim]^+$ cation are also found. The relatively small $[CH_3COO]^-$ anion binds to the hydrogen atoms of N1−H and N3−H groups in uracil, whereas the most acidic hydrogen atom (H2) of the bulky $[C_2mim]^+$ cation prefers to bind to the oxygen atoms of the carbonyl groups in uracil. The convergence of the results from the DFT calculations with the experimental NMR data, ^1H and ^{13}C NMR chemical shifts analysis, and $^1H-^1H$ NOESY NMR provides a high level of confidence in the quality of the dissolution mechanism proposed.

■ ASSOCIATED CONTENT

Supporting Information

^1H NMR and ^{13}C NMR spectra of uracil and $[C_2mim][CH_3COO]$ in DMSO-d_6 at 298 K. Effect of uracil concentration on the ^1H and ^{13}C NMR spectra of $[C_2mim][CH_3COO]$ in DMSO-d_6 and in situ. $^1H-^1H$ NOESY spectra of uracil/$[C_2mim][CH_3COO]$ mixtures in DMSO-d_6 at 298 K with a mixing time of 50 ms. This material is available free of charge via the Internet at http://pubs.acs.org.

■ AUTHOR INFORMATION

Corresponding Author

*Tel: (+351) 214 469 442. Fax: (+351) 214 411 277. E-mail: jmmda@itqb.unl.pt (J.M.M.A.); imarrucho@itqb.unl.pt (I.M.M.).

Notes

The authors declare no competing financial interest.

■ ACKNOWLEDGMENTS

The financial support from FCT/MEC (Portugal), through grants SFRH/BPD/65981/2009 (J.M.M.A.) and SFRH/BPD/84433/2012 (A.B.P.) and a contract under *Programa Ciência 2007* (I.M.M.) and through projects PTDC/EQU-EPR/104554/2008, PTDC/QUI-QUI/101794/2008, and PTDC/EQU-FTT/118800/2010 is gratefully acknowledged. The NMR spectrometers are part of the National NMR Network and were purchased in the framework of the National Program for Scientific Re-equipment, contract REDE/1517/RMN/2005, with funds from POCI 2010 (FEDER) and FCT/MEC.

■ REFERENCES

(1) *Ionic Liquids IIIA: Fundamentals, Progress, Challenges, and Opportunities: Properties and Structures*; Rogers, R. D., Seddon, K. R., Eds.; American Chemical Society: Washington, DC, 2005; Vol. *901*.

(2) Blanchard, L. A.; Brennecke, J. F. *Ind. Eng. Chem. Res.* **2001**, *40*, 287−292.

(3) Pereiro, A. B.; Araújo, J. M. M.; Oliveira, F. S.; Esperança, J. M. S. S.; Canongia Lopes, J. N.; Marrucho, I. M.; Rebelo, L. P. N. *J. Chem. Thermodynamics* **2012**, *55*, 29−36.

(4) Plechkova, N. V.; Seddon, K. R. *Chem. Soc. Rev.* **2008**, *37*, 123−150.

(5) Rogers, R. D.; Seddon, K. R. *Science* **2003**, *302*, 792−793.

(6) Baudequin, C.; Baudoux, J.; Levillain, J.; Cahard, D.; Gaumont, A.-C.; Plaquevent, J.-C. *Tetrahedron: Asymmetry* **2003**, *5*, 3081−3093.

(7) Armand, M.; Endres, F.; MacFarlane, D. R.; Ohno, H.; Scrosati, B. *Nat. Mater.* **2009**, *8*, 621−629.

(8) Pereiro, A. B.; Araújo, J. M. M.; Oliveira, F. S.; Bernardes, C. E. S.; Esperança, J. M. S. S.; Canongia Lopes, J. N.; Marrucho, I. M.; Rebelo, L. P. N. *Chem. Commun.* **2012**, *48*, 3656−3658.

(9) Dyson, P. J.; McIndoe, J. S.; Zhao, D. B. *Chem. Commun.* **2003**, 508−509.

(10) Garcia, H.; Ferreira, R.; Petkovic, M.; Ferguson, J. L.; Leitao, M. C.; Gunaratne, H. Q. N.; Seddon, K. R.; Rebelo, L. P. N.; Pereira, C. S. *Green Chem.* **2010**, *12*, 367−369.

(11) Majewski, P.; Pernak, A.; Grzymislawski, M.; Iwanik, K.; Pernak, J. *Acta Histochem.* **2003**, *105*, 135−142.

(12) Bernard, U. L.; Izgorodina, E. I.; MacFarlane, D. R. *J. Phys. Chem. C* **2010**, *114*, 20472−20478.

(13) Tsuzuki, S.; Tokuda, H.; Hayamizu, K.; Watanabe, M. *J. Phys. Chem. B* **2005**, *109*, 16474−16481.

(14) Zahn, S.; Uhlig, F.; Thar, J.; Spickermann, C.; Kirchner, B. *Angew. Chem., Int. Ed.* **2008**, *47*, 3639−3641.

(15) Rebelo, L. P. N.; Lopes, J. N.; Esperança, J. M. S. S.; Guedes, H. J. R.; Lachwa, J.; Najdanovic-Visak, V.; Visak, Z. P. *Acc. Chem. Res.* **2007**, *40*, 1114−1121.

(16) Shimizu, K.; Gomes, M. F. C.; Padua, A. A. H.; Rebelo, L. P. N.; Lopes, J. N. C. *J. Mol. Struct.: THEOCHEM* **2010**, *946*, 70−76.

(17) Lehmann, S. B. C.; Roatsch, M.; Schöppke, M.; Kirchner, B. *Phys. Chem. Chem. Phys.* **2010**, *12*, 7473−7486.

(18) Izgorodina, E. I.; MacFarlane, D. R. *J. Phys. Chem. B* **2011**, *115*, 14659−14667.

(19) Dhumal, N. R.; Kim, H. J.; Kiefer, J. *J. Phys. Chem. A* **2009**, *113*, 10397−10404.

(20) Youngs, T. G. A.; Holbrey, J. D.; Mullan, C. L.; Norman, S. E.; Lagunas, M. C.; D'Agostin, C.; Mantle, M. D.; Gladden, L. F.; Bowron, D. T.; Hardacre, C. *Chem. Sci.* **2011**, *2*, 1594−1605.

(21) Remsing, R. C.; Hernandez, G.; Swatloski, R. P.; Massefski, W. M.; Rogers, R. D.; Moyna, G. *J. Phys. Chem. B* **2008**, *112*, 11071−11078.

(22) Youngs, T. G. A.; Hardacre, C.; Holbrey, J. D. *J. Phys. Chem. B* **2007**, *111*, 13765−13774.

(23) Liu, H.; Sale, K. L.; Holmes, B. M.; Simmons, B. A.; Singh, S. *J. Phys. Chem. B* **2010**, *114*, 4293−4301.

(24) Zhao, H.; Jackson, L.; Song, Z.; Olubajo, O. *Tetrahedron: Asymmetry* **2006**, *17*, 2491−2498.

(25) Spange, S.; Reuter, A.; Vilsmeier, E.; Heinze, T.; Keutel, D.; Linert, W. *J. Polym. Sci., Part A* **1998**, *26*, 1945−1955.

(26) Ohno, H.; Fukaya, Y. *Chem. Lett.* **2009**, *38*, 2−7.

(27) *Electrochemical Aspects of Ionic Liquids*; Ohno, H., Ed.; Wiley-Interscience: New York, 2005.

(28) El Seoud, O. A.; Koschella, A.; Fidale, L. C.; Dorn, S.; Heinze, T. *Biomacromolecules* **2007**, *8*, 2629−2647.

(29) Araújo, J. M. M.; Ferreira, R.; Marrucho, I. M.; Rebelo, L. P. N. *J. Phys. Chem. B* **2011**, *115*, 10739−10749.

(30) Araújo, J. M. M.; Pereiro, A. B.; Alves, F.; Marrucho, I. M.; Rebelo, L. P. N. *J. Chem. Thermodyn.* **2013**, *57*, 1−8.

(31) Shiflett, M. B.; Kasprzak, D. J.; Junk, C. P.; Yokozeki, A. *J. Chem. Thermodyn.* **2008**, *40*, 25−31.

(32) Banks, J. F., Jr.; Whitehouse, C. M. *Int. J. Mass Spectrom. Ion Processes* **1997**, *162*, 163−172.

(33) Davies, R. G.; Gibson, V. C.; Hursthouse, M. B.; Ligth, M. E.; Marshall, E. L.; North, M.; Robson, D. A.; Thompson, I.; White, A. J. P.; Williams, D. J.; Williams, P. J. *J. Chem. Soc., Perkin Trans.* **2001**, *1*, 3365−3381.

(34) Baker, E. A.; Hayes, A. L.; Butler, R. C. *Pestic. Sci.* **1992**, *34*, 167−182.

(35) Zielenkiewicz, W.; Poznanski, J.; Zielenkiewicz, A. *J. Solution Chem.* **2000**, *29*, 757−769.

(36) Ganguly, S.; Kundu, K. K. *J. Phys. Chem.* **1993**, *41*, 10862−10867.

(37) De Pascuale, R. J. *Ind. Eng. Chem. Prod. Res. Dev.* **1978**, *17*, 278−286.

(38) *CRC Handbook of Chemistry and Physics*, 89th ed.; Lide, D. R. Ed.; CRC Press: Boca Raton, FL, 2008−2009.

(39) Sim, F.; St-Amant, A.; Papai, I.; Salahub, D. R. *J. Am. Chem. Soc.* **1992**, *114*, 4391−4400.

(40) Kim, K.; Jordan, K. D. *J. Phys. Chem.* **1994**, *98*, 10089−10094.

(41) Kristyan, S.; Pulay, P. *Chem. Phys. Lett.* **1994**, *229*, 175−180.

(42) Del Bene, J. E.; Person, W. B.; Szczepaniak, J. *J. Phys. Chem.* **1995**, *99*, 10705−10707.
(43) Chandra, A. K.; Nguyen, M. T. *J. Chem. Res.* **1997**, 216−217.
(44) Lee, C.; Yang, W.; Parr, R. G. *Phys. Rev. B* **1988**, *37*, 785−789.
(45) Becke, A. D. *J. Chem. Phys.* **1993**, *98*, 5648−5652.
(46) Frisch, M. J.; Trucks, G. W.; Schlegel, H. B.; Scuseria, G. E.; Robb, M. A.; Cheeseman, J. R.; Scalmani, G.; Barone, V.; Mennucci, B.; Petersson, G. A.; Nakatsuji, H.; Caricato, M.; Li, X.; Hratchian, H. P.; Izmaylov, A. F.; Bloino, J.; Zheng, G.; Sonnenberg, J. L.; Hada, M.; Ehara, M.; Toyota, K.; Fukuda, R.; Hasegawa, J.; Ishida, M.; Nakajima, T.; Honda, Y.; Kitao, O.; Nakai, H.; Vreven, T.; Montgomery, J. A., Jr.; Peralta, J. E.; Ogliaro, F.; Bearpark, M.; Heyd, J. J.; Brothers, E.; Kudin, K. N.; Staroverov, V. N.; Kobayashi, R.; Normand, J.; Raghavachari, K.; Rendell, A.; Burant, J. C.; Iyengar, S. S.; Tomasi, J.; Cossi, M.; Rega, N.; Millam, J. M.; Klene, M.; Knox, J. E.; Cross, J. B.; Bakken, V.; Adamo, C.; Jaramillo, J.; Gomperts, R.; Stratmann, R. E.; Yazyev, O.; Austin, A. J.; Cammi, R.; Pomelli, C.; Ochterski, J. W.; Martin, R. L.; Morokuma, K.; Zakrzewski, V. G.; Voth, G. A.; Salvador, P.; Dannenberg, J. J.; Dapprich, S.; Daniels, A. D.; Farkas, Ö.; Foresman, J. B.; Ortiz, J. V.; Cioslowski, J.; Fox, D. J. *Gaussian 09*; Gaussian, Inc.: Wallingford, CT, 2009.
(47) Boys, S. F.; Bernardi, F. *Mol. Phys.* **1970**, *19*, 553−566.
(48) White, J. C.; Davidson, E. R. *J. Chem. Phys.* **1990**, *93*, 8029−8035.
(49) Valiron, P.; Mayer, I. *Chem. Phys. Lett.* **1997**, *1997*, 46−55.
(50) Mierzwicki, K.; Latajka, Z. *Chem. Phys. Lett.* **2003**, *380*, 654−664.
(51) Leist, R.; Frey, J. A.; Ottiger, P.; Frey, H.-M.; Leutwyler, S.; Bachorz, R. A.; Klopper, W. *Angew. Chem., Int. Ed.* **2007**, *46*, 7449−7452.
(52) Pauling, L. *The Nature of the Chemical Bond*, 3rd ed.; Cornell University Press: New York, 1960.
(53) Baker, E. N.; Hubbard, R. E. *Prog. Biophys. Mol. Biol.* **1984**, *44*, 97−179.
(54) Arunan, E.; Desiraju, G. R.; Klein, R. A.; Sadlej, J.; Scheiner, S.; Alkorta, I.; Clary, D. C.; Crabtree, R. H.; Dannenberg, J. J.; Hobza, P.; Kjaergaard, H. G.; Legon, A. C.; Mennucci, B.; Nesbitt, D. *Pure Appl. Chem.* **2011**, *83*, 1637−1641.
(55) Chierotti, M. R.; Gobetto, R. *Chem. Commun.* **2008**, 1621−1634.
(56) Avent, A. G.; Chaloner, P. A.; Day, M. P.; Seddon, K. R.; Welton, T. *J. Chem. Soc., Dalton Trans.* **1994**, 3405−3413.
(57) Yashima, E.; Yamamoto, C.; Okamoto, Y. *J. Am. Chem. Soc.* **1996**, *118*, 4036−4048.
(58) McCormick, C. L.; Callais, P. A.; Hutchinson, B. H. *Macromolecules* **1985**, *18*, 2394−2401.
(59) Moulthrop, J. S.; Swatloski, R. P.; Moyna, G.; Rogers, R. D. *Chem. Commun.* **2005**, 1557−1559.
(60) Fort, D. A.; Swatloski, R. P.; Moyna, P.; Rogers, R. D.; Moyna, G. *Chem. Commun.* **2006**, 714−716.
(61) Zhang, J.; Zhang, H.; Wu, J.; Zhang, J.; He, J.; Xiang, J. *Phys. Chem. Chem. Phys.* **2010**, *12*, 1941−1947.
(62) Remsig, R. C.; Liu, Z. W.; Sergeyev, I.; Moyna, G. *J. Phys. Chem. B* **2006**, *112*, 7363−7369.
(63) Zhang, J.; Zhang, H.; Wu, J.; Zhang, J.; He, J.; Xiang, J. *Phys. Chem. Chem. Phys.* **2010**, *12*, 14829−14830.
(64) Zhang, S.; Qi, X.; Ma, X.; Lu, L.; Deng, Y. *J. Phys. Chem. B* **2010**, *114*, 3912−3920.
(65) Leontis, N. B.; Stombaugh, J.; Westhof, E. *Nucleic Acids Res.* **2002**, *30*, 3479−3531.
(66) Crick, F. H. C. *J. Mol. Biol.* **1966**, *19*, 548−555.
(67) Watson, J. D.; Crick, F. H. *Nature* **1953**, *171*, 737−738.
(68) Frey, J. A.; Müller, A.; Losada, M.; Leutwyler, S. *J. Phys. Chem. B* **2007**, *111*, 3534−3542.
(69) Kasende, O.; Zeegers-Huyskens, Th. *J. Phys. Chem.* **1984**, *88*, 2636−2641.
(70) Chandra, A. K.; Nguyen, M. T.; Zeegers-Huyskens, Th. *J. Chem. Soc., Faraday Trans.* **1998**, *94*, 1277−1280.
(71) Chandra, A. K.; Nguyen, M. T.; Zeegers-Huyskens, Th. *J. Phys. Chem. A* **1998**, *102*, 6010−6016.
(72) Mautner, M. *J. Am. Chem. Soc.* **1988**, *110*, 3071−3075.
(73) Mautner, M. *J. Am. Chem. Soc.* **1988**, *110*, 3075−3080.
(74) Nakanishi, K.; Suzuki, N.; Yamazaki, F. *Bull. Soc. Chim. Jpn.* **1961**, *34*, 53−57.
(75) Wempen, I.; Fox, J. J. *J. Am. Chem. Soc* **1964**, *86*, 2474−2477.
(76) Draiči′nský, M.; Holý,, A.; Jansa, P.; Kovačková, S.; Buděši′nský, M. *Eur. J. Org. Chem.* **2009**, *24*, 4117−4122.
(77) Zhai, C. P.; Wang, J. J.; Xuan, X. P.; Wang, H. Q. *Acta Phys.-Chim. Sin.* **2006**, *22*, 456−459.
(78) Crosthwaite, J. M.; Aki, S. N. V. K.; Maginn, E. J.; Brennecke, J. F. *J. Phys. Chem. B* **2004**, *108*, 5113−5119.
(79) Mele, A.; Tran, C. D.; De Paoli Lacerda, S. H. *Angew. Chem., Int. Ed.* **2003**, *42*, 4364−4366.
(80) Wu, B.; Liu, Y.; Zhang, Y. M.; Wang, H. P. *Chem.—Eur. J.* **2009**, *15*, 6889−6893.
(81) Ressmann, A. K.; Strassl, K.; Gaertner, P.; Zhao, B.; Greinerb, L.; Bica, K. *Green Chem.* **2012**, *14*, 940−944.
(82) Li, W.; Sun, N.; Stoner, B.; Jiang, X.; Lu, X.; Rogers, R. D. *Green Chem.* **2011**, *13*, 2038−2047.
(83) Besnard, M.; Cabaço, M. I.; Chávez, F. V.; Pinaud, N.; Sebastião, P. J.; Coutinho, J. A. P.; Mascetti, J.; Danten, Y. *J. Phys. Chem. A* **2012**, *116*, 4890−4901.
(84) Reeves, L. W. *Trans. Faraday Soc.* **1959**, *55*, 1684−1688.
(85) Fujii, Y.; Yamada, H.; Mizuta, M. *J. Phys. Chem.* **1988**, *92*, 6768−6772.
(86) Nyquist, R. A.; Dclark, T.; Streck, R. *Vibr. Spectrosc.* **1994**, *7*, 275−286.
(87) Génin, F.; Quilès, F.; Burneau, A. *Phys. Chem. Chem. Phys.* **2001**, *3*, 932−942.
(88) Neuhaus, D.; Williamson, M. P. *The Nuclear Overhauser Effect in Structural and Conformational Analysis*; Wiley-VCH: New York, 2000.
(89) Canet, D. *Nuclear Magnetic Resonance: Concepts and Methods*; Wiley: New York, 1996.
(90) Van de Ven, F. J. M. *Multidimensional NMR in Liquids: Basic Principles and Experimental Methods*; Wiley: New York, 1995.